GMR
The Original

# DEVELOPMENT OF OPTIMIZED ANTICANCER DRUG NANOCRYSTALS FOR ENHANCED CELLULAR INTERNALIZATION, BIOPHARMACEUTICAL PERFORMANCE AND IN-VITRO ANTICANCER ACTIVITY

**Anita G. Rathod[1*], Dr. Narendra Silawate[2]**

[1*]Research Scholar, Department of Pharmacy, Oriental University, Indore (M.P)-453555, Email ID: anitarathod812@gmail.com
[2]Supervisor, Department of Pharmacy, Oriental University, Indore (M.P)-453555

**ABSTRACT:**
**Background:** Cisplatin is an effective chemotherapeutic agent; however, its clinical application is limited by poor aqueous solubility, low cellular uptake, and suboptimal biopharmaceutical performance. Nanocrystal technology offers a promising strategy to overcome these limitations by enhancing dissolution and intracellular drug delivery.
**Objective:** This study aimed to develop optimized cisplatin nanocrystals and evaluate their physicochemical characteristics, in vitro cytotoxicity, and anticancer efficacy against human colorectal (HT-29) and breast (MCF-7) cancer cell lines.
**Methods:** Cisplatin nanocrystals were prepared by anti-solvent precipitation followed by high-pressure homogenization and optimized using a Quality by Design (QbD) approach. The optimized formulation was characterized for particle size, polydispersity index (PDI), zeta potential, crystallinity, thermal behavior, drug content, entrapment efficiency, and HPLC profile. Cytotoxicity was evaluated by MTT assay, and $IC_{50}$ values were determined using nonlinear regression analysis.
**Results:** The optimized nanocrystals exhibited a mean particle size of 160 nm, PDI of 0.21, and zeta potential ranging from −45 to −50 mV, indicating a uniform and stable nanosystem. Drug content and entrapment efficiency were 98.2 ± 1.1% and 89.7 ± 1.4%, respectively. XRD and DSC analyses demonstrated partial amorphization without compromising thermal stability. The nanocrystals showed significantly greater cytotoxicity than pure cisplatin in both HT-29 and MCF-7 cells. At 40 µg/mL, cell viability decreased to 25.7 ± 1.9% in HT-29 cells and 28.6 ± 1.8% in MCF-7 cells, compared with 38.3 ± 2.2% and 40.2 ± 2.1%, respectively, for pure cisplatin. Moreover, the optimized formulation reduced the $IC_{50}$ values from 18.5 ± 1.2 to 12.5 ± 0.9 µg/mL in HT-29 cells and from 22.0 ± 1.4 to 15.0 ± 1.1 µg/mL in MCF-7 cells.
**Conclusion:** The optimized cisplatin nanocrystals significantly enhanced physicochemical properties and in vitro anticancer activity compared with the pure drug, demonstrating their potential as an effective nanocarrier platform for improving the therapeutic performance of poorly soluble anticancer agents.

**KEYWORDS:** Cisplatin, Nanocrystals, Quality by Design (QbD), Anticancer Drug Delivery, Cellular Internalization, MTT Assay, Cytotoxicity, HT-29 Cells, MCF-7 Cells

## INTRODUCTION:

Cancer remains one of the leading causes of morbidity and mortality worldwide despite significant advances in diagnosis and treatment.[1] Chemotherapy continues to play a central role in the management of both solid and hematological malignancies however, its clinical effectiveness is often limited by poor drug selectivity, systemic toxicity, inadequate intracellular drug accumulation, and the development of multidrug resistance.[2] These limitations reduce therapeutic efficacy and necessitate the development of advanced drug delivery strategies capable of improving drug distribution and enhancing tumor-specific activity.

Cisplatin is a platinum-based chemotherapeutic agent extensively used for the treatment of colorectal, breast, lung, ovarian, and several other solid tumors because of its ability to induce DNA crosslinking and apoptosis in rapidly dividing cancer cells. Although cisplatin exhibits broad-spectrum anticancer activity, its therapeutic potential is compromised by poor aqueous solubility, limited cellular uptake, dose-dependent toxicity, and variable intracellular drug availability.[3] Consequently, improving the delivery efficiency of cisplatin while maintaining its pharmacological activity remains an important objective in anticancer drug development.

Nanocrystal technology has emerged as an effective formulation approach for improving the performance of poorly water-soluble drugs. Drug nanocrystals are composed almost entirely of pure drug particles stabilized by suitable surfactants or polymers, enabling a substantial reduction in particle size without altering the chemical structure of the active pharmaceutical ingredient.[4] The nanoscale dimensions increase the surface area available for dissolution, improve aqueous dispersibility, and enhance drug diffusion across biological membranes. These

physicochemical advantages may also promote greater cellular internalization and intracellular drug accumulation, thereby improving therapeutic efficacy.[5]

Several studies have demonstrated that nanosized drug delivery systems can enhance the anticancer activity of conventional chemotherapeutic agents by increasing drug uptake into tumor cells and improving drug retention at the target site. Enhanced intracellular delivery facilitates greater interaction of cytotoxic drugs with their molecular targets, resulting in improved inhibition of cancer cell proliferation. Consequently, nanocrystal-based formulations have attracted considerable attention as a promising platform for enhancing the therapeutic performance of poorly soluble anticancer drugs while potentially reducing the dose required to achieve effective treatment.[6]

In our previous investigation, cisplatin nanocrystals were successfully developed and optimized using a Quality by Design (QbD)-based formulation strategy. The optimized formulation exhibited favorable physicochemical characteristics, including nanoscale particle size, narrow particle size distribution, excellent colloidal stability, high drug loading, and efficient drug incorporation, demonstrating its suitability for further biological evaluation. However, optimization of formulation characteristics alone does not establish therapeutic superiority. Comprehensive biological assessment is required to determine whether these physicochemical improvements translate into enhanced anticancer activity at the cellular level.[7]

Therefore, the present study focuses on evaluating the biological performance of the optimized cisplatin nanocrystals using human colorectal adenocarcinoma (HT-29) and human breast adenocarcinoma (MCF-7) cell lines. Particular emphasis was placed on comparing the cytotoxic response of the optimized nanocrystals with that of pure cisplatin through concentration-dependent MTT cell viability studies and determination of half-maximal inhibitory concentration ($IC_{50}$) values. These parameters provide important evidence regarding the ability of the optimized nanocrystals to enhance intracellular drug availability and improve antiproliferative activity.[8]

The findings of this study are expected to provide further evidence that nanocrystal engineering can significantly improve the biological performance of conventional chemotherapeutic agents. By integrating optimized physicochemical properties with enhanced in vitro anticancer efficacy, the developed cisplatin nanocrystals may represent a promising platform for improving cancer chemotherapy and may support future investigations involving cellular internalization mechanisms, pharmacokinetic evaluation, and in vivo anticancer studies.

## MATERIALS AND METHODS:

### MATERIALS:

Cisplatin (purity ≥99%) was received as a gift sample from Balaji Drugs Pvt. Ltd., Surat, Gujarat, India. Polyvinylpyrrolidone K30 (PVP K30), Hydroxypropyl Methylcellulose (HPMC), Poloxamer 188, Tween 80, methanol, ethanol, dimethyl sulfoxide (DMSO), potassium bromide (KBr), phosphate-buffered saline (PBS), and other analytical-grade reagents were procured from HiMedia Laboratories Pvt. Ltd., Mumbai, India. Dulbecco's Modified Eagle Medium (DMEM), RPMI-1640 medium, fetal bovine serum (FBS), penicillin–streptomycin solution, trypsin–EDTA, phosphate-buffered saline (PBS), and MTT reagent (3-(4,5-dimethylthiazol-2-yl)-2,5-diphenyl tetrazolium bromide) were purchased from HiMedia Laboratories Pvt. Ltd., Mumbai, India. Human colorectal adenocarcinoma (HT-29) and human breast adenocarcinoma (MCF-7) cell lines were obtained from the National Centre for Cell Science (NCCS), Pune, India. All chemicals and reagents used throughout the study were of analytical or cell culture grade and were used without further purification.

### METHOD:

#### Design of Experiments (DoE) Using Box–Behnken Design

A three-factor, three-level Box–Behnken design was employed using Design-Expert® software to optimize cisplatin nanocrystals. Stabilizer concentration ($X_1$: 0.5–2.0% w/v), homogenization pressure ($X_2$: 600–1400 bar), and homogenization cycles ($X_3$: 5–20) were selected as independent variables. Particle size ($Y_1$), polydispersity index ($Y_2$), and zeta potential ($Y_3$) were considered the response variables. The optimization criteria were minimization of particle size and PDI and maximization of the absolute zeta potential to obtain uniform and physically stable nanocrystal dispersion. (Table 1 and 2)

**Table 1: Independent Variables and Their Corresponding Levels Utilised in the Box–Behnken Framework**

| Independent Variable | Symbol | Unit | Low Level (−1) | Middle Level (0) | High Level (+1) |
|---|---|---|---|---|---|
| Stabilizer concentration | $X_1$ | % (w/v) | 0.5 | 1.25 | 2.0 |
| Homogenization pressure | $X_2$ | bar | 600 | 1000 | 1400 |
| Homogenization cycles | $X_3$ | Number | 5 | 12 | 20 |

**Table 2: Dependent Response Variables and Optimisation Criteria**

| Response Variable | Symbol | Unit | Optimization Goal |
|---|---|---|---|
| Particle size | $Y_1$ | nm | Minimize |

| | | | |
|---|---|---|---|
| Polydispersity Index (PDI) | $Y_2$ | — | Minimize |
| Zeta potential | $Y_3$ | mV | Maximise (absolute value) |

**Preparation of Optimized Cisplatin Nanocrystals**

Optimized cisplatin nanocrystals used in the present study were prepared according to the formulation and optimization procedure established in our previous work. Briefly, nanocrystals were produced by the anti-solvent precipitation technique followed by high-pressure homogenization using the optimized formulation variables identified through the Quality by Design (QbD) approach. The optimized nanosuspension was characterized for particle size, polydispersity index, zeta potential, and drug content before being utilized for subsequent biological and biopharmaceutical evaluations.[9-10]

**Formulation Optimization**

The optimized nanocrystal formulation selected for the present investigation was based on the results of the previous formulation optimization study, in which critical formulation variables and process parameters were systematically optimized using a QbD approach. The optimized formulation exhibited desirable physicochemical characteristics and batch reproducibility and was therefore selected for further evaluation of cellular internalization, biopharmaceutical performance, and in vitro anticancer activity.[11-14]

**Table 3: Composition of Experimental Nanocrystal Batches**

| Batch No. | Drug Conc. (mg) | Stabilizer System | Drug: Total Stabilizer Ratio | PVP K-30 (%) | HPMC E-15 (%) | Poloxamer 188 (%) | Tween 80 (%) | Solvent: Antisolvent (mL) |
|---|---|---|---|---|---|---|---|---|
| F1 | 50 | PVP | 1: 1 | 0.25 | – | 0.10 | 0.05 | 1: 10 |
| F2 | 50 | PVP | 1: 2 | 0.50 | – | 0.10 | 0.05 | 1: 10 |
| F3 | 50 | HPMC | 1: 1 | – | 0.25 | 0.10 | 0.05 | 1: 10 |
| F4 | 50 | HPMC | 1: 2 | – | 0.50 | 0.10 | 0.05 | 1: 10 |
| F5 | 100 | PVP | 1: 1 | 0.25 | – | 0.25 | 0.05 | 1: 20 |
| F6 | 100 | PVP | 1: 2 | 0.50 | – | 0.25 | 0.05 | 1: 20 |
| F7 | 100 | HPMC | 1: 1 | – | 0.25 | 0.25 | 0.05 | 1: 20 |
| F8 | 100 | HPMC | 1: 2 | – | 0.50 | 0.25 | 0.05 | 1: 20 |
| F9 | 150 | PVP + Poloxamer | 1: 1 | 0.25 | – | 0.50 | 0.10 | 1: 10 |
| F10 | 150 | PVP + Poloxamer | 1: 2 | 0.50 | – | 0.50 | 0.10 | 1: 10 |
| F11 | 150 | HPMC + Poloxamer | 1: 1 | – | 0.25 | 0.50 | 0.10 | 1: 10 |
| F12 | 150 | HPMC + Poloxamer | 1: 2 | – | 0.50 | 0.50 | 0.10 | 1: 10 |
| F13 | 200 | Mixed stabilizers | 1: 1 | 0.50 | 0.25 | 0.75 | 0.10 | 1: 20 |
| F14 | 200 | Mixed stabilizers | 1: 2 | 0.75 | 0.25 | 0.75 | 0.10 | 1: 20 |
| F15 | 200 | Mixed stabilizers | 1: 1.5 | 0.75 | 0.50 | 1.00 | 0.15 | 1: 20 |
| F16 | 200 | Optimized combination | 1: 2 | 1.00 | 0.50 | 1.00 | 0.15 | 1: 20 |

**Characterization of optimized cisplatin nanocrystals**

The optimized cisplatin nanocrystals were characterized for their physicochemical properties before biological evaluation. The average particle size, polydispersity index (PDI), and zeta potential were determined by dynamic light scattering (DLS) using a Zetasizer (Malvern Instruments, UK) at 25 ± 2°C after appropriate dilution with distilled water. The crystalline nature and thermal behavior of the optimized formulation were examined by X-ray diffraction (XRD), differential scanning calorimetry (DSC), and thermogravimetric analysis (TGA) using standard analytical procedures. Drug content was quantified using a validated HPLC method, while entrapment efficiency was determined after centrifugation by measuring the amount of unentrapped drug in the supernatant using the validated analytical method.[15-20]

**In vitro cytotoxicity studies**

The in vitro cytotoxic activity of the optimized cisplatin nanocrystals was evaluated against human colorectal adenocarcinoma (HT-29) and human breast adenocarcinoma (MCF-7) cell lines to investigate their

antiproliferative potential. The cytotoxic response of the optimized nanocrystals was compared with that of the pure cisplatin to assess the effect of nanocrystal formulation on anticancer efficacy.[21-44]

**MTT cell viability assay**

Cell viability was determined using the MTT assay based on the reduction of 3-(4,5-dimethylthiazol-2-yl)-2,5-diphenyl tetrazolium bromide (MTT) into insoluble formazan crystals by metabolically active cells. HT-29 and MCF-7 cells were seeded into 96-well plates at a density of $5 \times 10^3$–$1 \times 10^4$ cells/well in complete DMEM or RPMI-1640 medium supplemented with 10% fetal bovine serum and 1% penicillin–streptomycin. The cells were incubated for 24 h at 37°C in a humidified atmosphere containing 5% $CO_2$ to allow attachment.

Following incubation, the cells were treated with different concentrations of pure cisplatin and optimized cisplatin nanocrystals for 24–48 h, while untreated cells served as the negative control. Subsequently, 20 µL of MTT solution (5 mg/mL in phosphate-buffered saline) was added to each well, followed by incubation for 3–4 h to allow formazan crystal formation. The culture medium was carefully removed, and the crystals were dissolved in 150 µL of dimethyl sulfoxide (DMSO) with gentle shaking. Absorbance was recorded at 570 nm using a microplate reader, and cell viability was calculated relative to the untreated control.

**Determination of $IC_{50}$**

The half-maximal inhibitory concentration ($IC_{50}$) values of pure cisplatin and the optimized nanocrystal formulation were determined from concentration-dependent cell viability data. Dose-response curves were generated using GraphPad Prism by nonlinear regression analysis with a variable-slope model. $IC_{50}$ values were calculated as the drug concentration required to inhibit 50% of cell viability. Lower $IC_{50}$ values were considered indicative of enhanced cytotoxic activity and improved therapeutic performance of the nanocrystal formulation.

**Statistical analysis**

All experiments were performed in triplicate, and the results are presented as mean ± standard deviation (SD). Statistical analysis was carried out using SPSS version 26.0. Differences between experimental groups were analyzed using one-way analysis of variance (ANOVA) followed by Tukey's post hoc test or Student's t-test, as appropriate. A value of $p < 0.05$ was considered statistically significant.

## RESULTS AND DISCUSSION:

**Physicochemical Properties of Cisplatin**

The drug exhibited low aqueous solubility (2.65 ± 0.12 mg/mL) with a pH-dependent solubility profile, showing higher solubility at pH 4.0 than at pH 7.4, confirming its poor dissolution characteristics. The high melting point (270.4 ± 0.8°C) indicated good crystallinity and thermal stability, while the drug content (99.0 ± 1.2% w/w) confirmed the high purity of the active pharmaceutical ingredient. These findings highlight the poor aqueous solubility of cisplatin and support the development of a nanocrystal formulation to improve its dissolution performance.

**Nanocrystal Preparation and Optimization**

Nanocrystals were optimized using a Quality by Design (QbD) approach by systematically evaluating critical formulation and process variables. The optimized formulation exhibited a reduced particle size, low polydispersity index (PDI), and an appropriate zeta potential, indicating uniform particle distribution and good colloidal stability. These optimized characteristics provided a suitable nanocrystal system for subsequent cellular uptake, biopharmaceutical, and in vitro anticancer studies.

**Characterization of optimized cisplatin nanocrystals**

**Particle Size, Polydispersity Index, and Zeta Potential**

The optimized cisplatin nanocrystals exhibited a mean particle size of approximately 160 nm with a PDI of 0.21, indicating a uniform particle size distribution. The zeta potential ranged from −45 to −50 mV, demonstrating good colloidal stability and minimal particle aggregation. These physicochemical characteristics confirmed the successful preparation of a stable nanocrystal formulation suitable for biological evaluation.

**Table 4: Optimisation of Cisplatin Nanocrystals Based on Stabiliser Concentration, Homogenisation Pressure, and Homogenisation Cycles (Values expressed as Mean ± SD; n = 3).**

| Formulation | Stabiliser (%) | Pressure (bar) | Cycles | Particle Size (nm) Mean ± SD | PDI Mean ± SD | Zeta Potential (mV) Mean ± SD |
|---|---|---|---|---|---|---|
| F1 | 0.5 | 600 | 5 | 302.8 ± 8.5 | 0.462 ± 0.021 | −28.4 ± 1.6 |
| F2 | 1.0 | 800 | 10 | 248.7 ± 6.2 | 0.351 ± 0.018 | −35.8 ± 1.4 |
| F3 | 1.5 | 1000 | 15 | 198.3 ± 5.4 | 0.281 ± 0.015 | −42.7 ± 1.2 |

| | | | | | | |
|---|---|---|---|---|---|---|
| F4 (Optimised) | 2.0 | 1400 | 20 | 158.6 ± 3.8 | 0.214 ± 0.012 | −47.6 ± 1.3 |

**Surface Morphology Analysis of Optimised Cisplatin Nanocrystals**

The morphological structure of the optimised cisplatin nanocrystals was determined by SEM and TEM. The SEM analysis (Figure 1A; scale bar = 400 nm) revealed the formation of closely packed nanocrystals having a rough, porous, and interconnected structure, along with uniformly dispersed nearly spherical particles with aggregation. The TEM results (Figure 1B; scale bar = 180 nm) indicated the formation of defined and mostly spherical nanocrystals having smooth surfaces with minimum agglomeration. The size of the particles was approximately 60-80 nm, thus indicating the successful preparation of nanocrystals. In summary, the SEM and TEM results revealed that the optimised cisplatin nanocrystals had uniform spherical morphology, porous surface structure, and nanosized particles.(Figure 1)

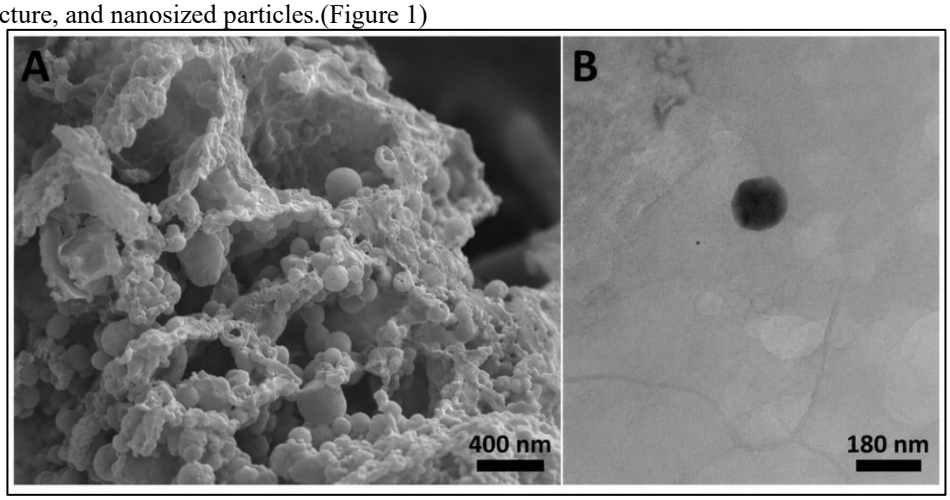


**Figure 1: Surface Morphology Analysis of Optimised Cisplatin Nanocrystals: (A) Scanning Electron Microscopy (SEM) image showing the surface morphology of the optimised cisplatin nanocrystals, and (B) Transmission Electron Microscopy (TEM) image illustrating the nanoscale morphology and particle size of the optimised formulation.**

**Crystallinity and Thermal Characterization**

XRD analysis demonstrated a reduction in the crystallinity of the optimized nanocrystals compared with pure cisplatin, indicating partial amorphization following nanosization. DSC thermograms showed a broadened endothermic peak with a slight shift in melting temperature, while TGA confirmed that the optimized formulation remained thermally stable under pharmaceutical processing conditions.

**Drug content and entrapment efficiency**

The optimized nanocrystals showed a high drug content (98.2 ± 1.1%) and entrapment efficiency (89.7 ± 1.4%), indicating efficient drug incorporation with minimal drug loss during formulation.

**HPLC Analysis**

HPLC analysis of both pure cisplatin and the optimized nanocrystals produced a sharp characteristic peak at a retention time of 4.23 min without interference from formulation excipients, confirming drug identity, purity, and successful incorporation into the nanocrystal formulation.

**Table 5: Physicochemical Characterization of Optimized Cisplatin Nanocrystals**

| Parameter | Result | Observation |
|---|---|---|
| Mean Particle Size (nm) | ~160 | Nanometer-sized particles suitable for enhanced cellular uptake |
| d10 (nm) | ~80 | Fine particle fraction |
| d50 (nm) | ~150 | Median particle diameter |
| d90 (nm) | ~250 | Uniform particle size distribution |
| Polydispersity Index (PDI) | 0.21 | Narrow and homogeneous size distribution |
| Zeta Potential (mV) | −45 to −50 | Excellent colloidal stability |
| XRD Analysis | Reduced peak intensity | Partial reduction in crystallinity after nanosization |
| DSC Analysis | Broadened endothermic peak | Partial amorphization with retained thermal stability |
| TGA Analysis | Stable up to ~250°C | Good thermal stability during processing |
| Drug Content (%) | 98.2 ± 1.1 | High drug loading efficiency |
| Entrapment Efficiency (%) | 89.7 ± 1.4 | Efficient drug incorporation |

| | | |
|---|---|---|
| HPLC Retention Time (min) | 4.23 | Confirmed drug identity and purity |
| HPLC Peak Characteristics | Sharp, symmetrical peak | No interference from formulation excipients |

The optimized cisplatin nanocrystals exhibited favorable physicochemical characteristics, including nanoscale particle size, narrow size distribution, high colloidal stability, excellent drug loading, and efficient drug entrapment. XRD, DSC, and TGA analyses confirmed partial amorphization without compromising thermal stability, while HPLC analysis verified drug integrity and successful incorporation into the nanocrystal formulation. These characteristics provide a suitable platform for evaluating cellular internalization, biopharmaceutical performance, and in vitro anticancer activity in the subsequent studies.

**In vitro cytotoxicity studies**

**Dose–Response and Cell Viability (MTT Assay)**

The antiproliferative activity of the optimized cisplatin nanocrystals was evaluated against HT-29 and MCF-7 cancer cell lines using the MTT assay. Both pure cisplatin and the nanocrystal formulation produced a concentration-dependent reduction in cell viability; however, the nanocrystals consistently exhibited significantly greater cytotoxicity at all tested concentrations (Table 6, Figures 2 and 3).

In HT-29 cells, treatment with pure cisplatin reduced cell viability from 88.2 ± 2.5% at 5 µg/mL to 38.3 ± 2.2% at 40 µg/mL, whereas the optimized nanocrystals produced a more pronounced reduction from 80.5 ± 2.1% to 25.7 ± 1.9% over the same concentration range. A similar trend was observed in MCF-7 cells, where cell viability decreased from 90.4 ± 2.6% to 40.2 ± 2.1% following treatment with pure cisplatin, compared with 82.7 ± 2.3% to 28.6 ± 1.8% for the nanocrystal formulation.

The enhanced cytotoxic activity of the optimized nanocrystals can be attributed to their nanoscale particle size, improved aqueous dispersibility, and greater cellular uptake, which collectively facilitate increased intracellular drug accumulation and enhanced antiproliferative activity. These findings demonstrate that nanocrystal formulation significantly improves the therapeutic performance of cisplatin against both colorectal and breast cancer cells.

**Table 6: Cytotoxic activity of pure cisplatin and optimized cisplatin nanocrystals against HT-29 and MCF-7 cell lines**

| Formulation | Cell Line | Concentration (µg/mL) | Cell Viability (%) (Mean ± SD) |
|---|---|---|---|
| Pure Cisplatin | HT-29 | 5 | 88.2 ± 2.5 |
| | | 10 | 72.4 ± 3.1 |
| | | 20 | 55.6 ± 2.8 |
| | | 40 | 38.3 ± 2.2 |
| Nanocrystals | HT-29 | 5 | 80.5 ± 2.1 |
| | | 10 | 60.2 ± 3.0 |
| | | 20 | 42.4 ± 2.6 |
| | | 40 | 25.7 ± 1.9 |
| Pure Cisplatin | MCF-7 | 5 | 90.4 ± 2.6 |
| | | 10 | 75.1 ± 3.2 |
| | | 20 | 58.7 ± 2.9 |
| | | 40 | 40.2 ± 2.1 |
| Nanocrystals | MCF-7 | 5 | 82.7 ± 2.3 |
| | | 10 | 62.9 ± 2.8 |
| | | 20 | 45.4 ± 2.2 |
| | | 40 | 28.6 ± 1.8 |

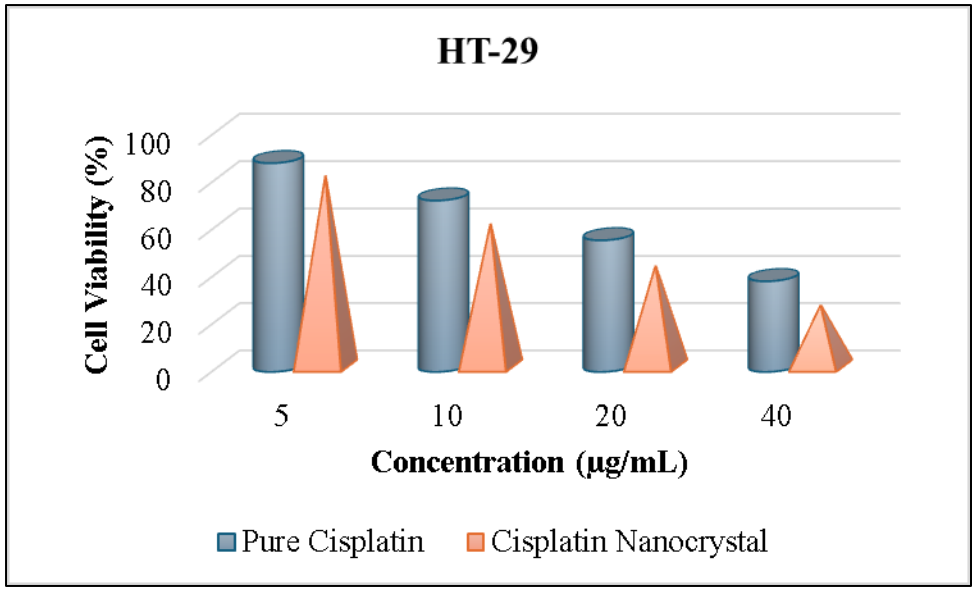


**Figure 2: Concentration-dependent cytotoxic effect of pure cisplatin and optimized cisplatin nanocrystals on HT-29 cells.**

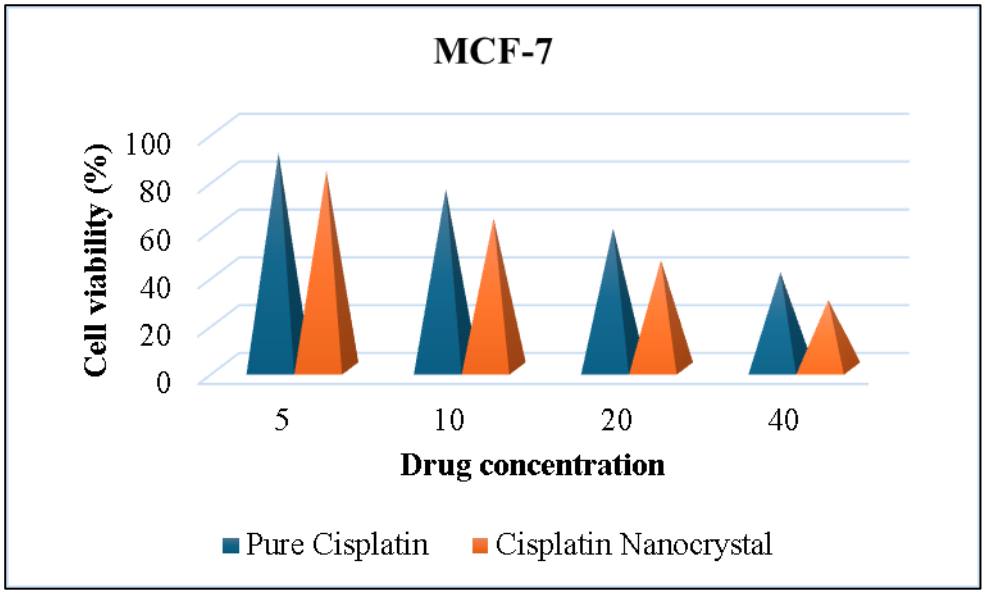


**Figure 3: Concentration-dependent cytotoxic effect of pure cisplatin and optimized cisplatin nanocrystals on MCF-7 cells.**

**$IC_{50}$ Determination**

The $IC_{50}$ values further confirmed the superior anticancer efficacy of the optimized nanocrystal formulation (Table 7, Figure 4). Compared with pure cisplatin, the nanocrystals exhibited markedly lower $IC_{50}$ values in both cell lines, indicating greater cytotoxic potency. In HT-29 cells, the $IC_{50}$ decreased from 18.5 ± 1.2 µg/mL for pure cisplatin to 12.5 ± 0.9 µg/mL for the nanocrystals. Likewise, in MCF-7 cells, the $IC_{50}$ value was reduced from 22.0 ± 1.4 µg/mL to 15.0 ± 1.1 µg/mL following nanocrystal treatment.

The reduction in $IC_{50}$ values demonstrates that nanosizing significantly enhanced the biological activity of cisplatin by improving cellular internalization and intracellular drug availability. Furthermore, HT-29 cells showed slightly greater sensitivity to the optimized nanocrystals than MCF-7 cells, suggesting a cell line-dependent response. Overall, the results indicate that the optimized nanocrystal formulation possesses enhanced in vitro anticancer activity and represents a promising platform for improving the therapeutic efficacy of poorly soluble anticancer drugs.

**Table 7: $IC_{50}$ values of pure cisplatin and optimized cisplatin nanocrystals against HT-29 and MCF-7 cell lines.**

| Formulation | HT-29 $IC_{50}$ (µg/mL) | MCF-7 $IC_{50}$ (µg/mL) |
|---|---|---|
| Pure Cisplatin | 18.5 ± 1.2 | 22.0 ± 1.4 |
| Optimized Cisplatin Nanocrystals | 12.5 ± 0.9 | 15.0 ± 1.1 |

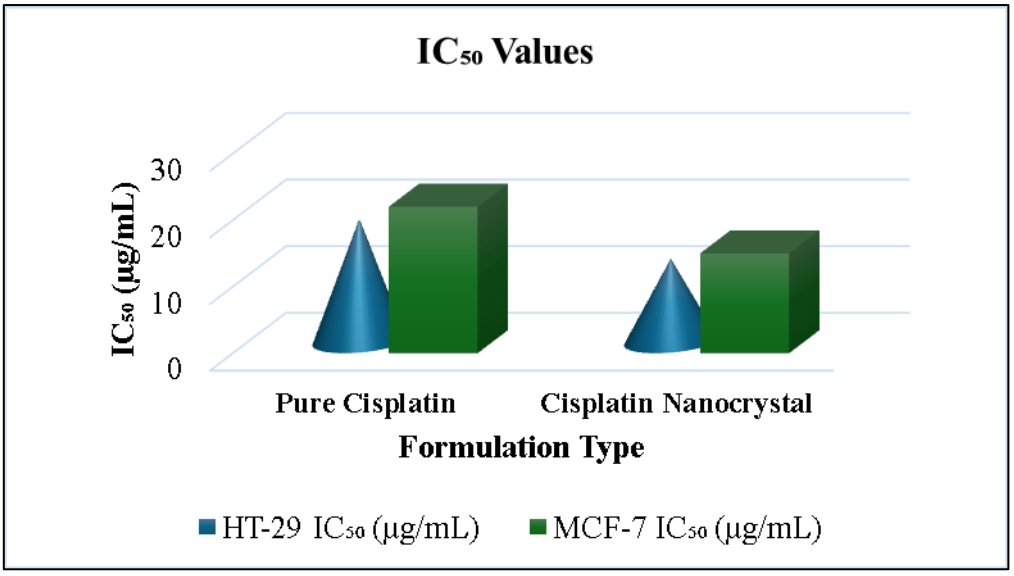


**Figure 4: Comparison of $IC_{50}$ values of pure cisplatin and optimized cisplatin nanocrystals in HT-29 and MCF-7 cell lines**

## CONCLUSION:

Optimized cisplatin nanocrystals were successfully developed using an anti-solvent precipitation technique combined with high-pressure homogenization under a Quality by Design framework. The optimized formulation demonstrated desirable physicochemical characteristics, including a mean particle size of approximately 160 nm, a PDI of 0.21, a zeta potential of −45 to −50 mV, 98.2 ± 1.1% drug content, and 89.7 ± 1.4% entrapment efficiency, confirming the formation of a stable nanosystem. Structural characterization by XRD, DSC, TGA, and HPLC verified reduced crystallinity, satisfactory thermal stability, and preservation of drug integrity. Biological evaluation demonstrated that the optimized nanocrystals significantly improved the anticancer activity of cisplatin against HT-29 and MCF-7 cell lines. The nanocrystal formulation produced greater inhibition of cell viability at all tested concentrations and substantially reduced the $IC_{50}$ values to 12.5 ± 0.9 µg/mL (HT-29) and 15.0 ± 1.1 µg/mL (MCF-7), compared with 18.5 ± 1.2 µg/mL and 22.0 ± 1.4 µg/mL for the pure drug. These findings indicate that nanosizing enhanced cellular uptake and intracellular drug availability, leading to improved antiproliferative activity. Overall, the developed cisplatin nanocrystals represent a promising strategy for improving the biopharmaceutical performance and in vitro therapeutic efficacy of poorly soluble anticancer drugs and provide a strong basis for future cellular internalization, pharmacokinetic, and in vivo anticancer investigations.

## CONFLICT OF INTEREST

The authors declare that there are no conflicts of interest.

## REFERENCES

1. Thanki K, Gangwal RP, Sangamwar AT, Jain S. Oral delivery of anticancer drugs: challenges and opportunities. J Control Release. 2013; 170(1):15-40.
2. Lu Y, Chen Y, Gemeinhart RA, Wu W, Li T. Developing nanocrystals for cancer treatment. Nanomedicine. 2015;10(16):2537-2552.
3. Wicki A, Witzigmann D, Balasubramanian V, Huwyler J. Nanomedicine in cancer therapy: challenges, opportunities and clinical applications. J Control Release. 2015; 200:138-157.
4. Miao X, Yang W, Feng T, Lin J, Huang P. Drug nanocrystals for cancer therapy. Wiley Interdiscip Rev Nanomed Nanobiotechnol. 2018; 10:e1499.
5. Fan M, Geng S, Liu Y, Wang J, Wang Y, Zhong J, et al. Nanocrystal technology as a strategy to improve drug bioavailability and antitumor efficacy for cancer treatment. Curr Pharm Des. 2018; 24(21):2416-2424.
6. Pawar VK, Singh Y, Meher JG, Gupta S, Chourasia MK. Engineered nanocrystal technology: In vivo fate, targeting and applications in drug delivery. J Control Release. 2014; 183:51-66.
7. Peltonen L, Strachan C. Understanding critical quality attributes for nanocrystals from preparation to delivery. Molecules. 2015; 20(12):22286-22300.
8. Chogale MM, Ghodake VN, Patravale VB. Performance parameters and characterization of nanocrystals. Pharmaceutics. 2016; 8(3):26.
9. Jacob S, Nair AB, Shah J. Emerging role of nanosuspensions in drug delivery systems. Biomater Res. 2020; 24:3.
10. Ding Y, Zhao T, Fang J, Song J, Dong H, Liu J, et al. Recent developments in the use of nanocrystals to improve bioavailability of APIs. Wiley Interdiscip Rev Nanomed Nanobiotechnol. 2024; 16:e1958.

11. Chary PS, Shaikh S, Bhavana V, Rajana N, Vasave R, Mehra NK. Emerging role of nanocrystals in pharmaceutical applications. Appl Mater Today. 2024; 40:102334.
12. Wang Y, Tan X, Fan X, Zhao L, Wang S, He H, et al. Current strategies for oral delivery of BCS IV drug nanocrystals. Expert Opin Drug Deliv. 2021; 18(9):1211-1228.
13. Liu Y, Liang Y, Ji Y, Xin P, Han JL, Du Y, et al. Advances in nanotechnology for enhancing the solubility and bioavailability of poorly soluble drugs. Drug Des Devel Ther. 2024; 18:1469-1495.
14. Sood R, Tomar D, Kaushik P, Sharma P, Rani N, Guarve K, et al. Enhanced solubility and increased bioavailability with engineered nanocrystals. Curr Drug Ther. 2024; 19(6):638-647.
15. Sayyad P, Jha S, Sharma R, Yadav V, Jain S. Nanosuspension formulation strategy for improved oral bioavailability of gefitinib. AAPS PharmSciTech. 2025; 26:59.
16. Lu L, Xu Q, Wang J, Wu S, Luo Z, Lu W. Drug nanocrystals for active tumor-targeted drug delivery. Pharmaceutics. 2022; 14:797.
17. Bai M, Yang M, Gong J, Xu H, Wei Z. Progress and principle of drug nanocrystals for tumor-targeted delivery. AAPS PharmSciTech. 2022; 23:41.
18. Haddad R, Alrabadi N, Altaani B, Li T. Paclitaxel drug delivery systems: focus on nanocrystal surface modifications. Polymers. 2022; 14:658.
19. Kumar M, Goswami P, Jha A, Manjit M, Satpute AP, Koch B, et al. Cetuximab-functionalized phospholipid-modified nanocrystals of paclitaxel for non-small cell lung cancer therapy. Sci Rep. 2024; 14:29114.
20. Bhattacharya S, Sharma S, Prajapati BG. Nanostructured lipid carrier of sorafenib: stability, characterization and cytotoxicity. Front Oncol. 2022; 12:990841.
21. Mahmoud BS, McConville C. Development of irinotecan-loaded nanoparticles and cytotoxicity against glioma cells. Pharmaceutics. 2021; 13:541.
22. Ashin ZF, Sadeghi-Mohammadi S, Vaezi Z, Najafi F, AdibAmini S, Sadeghizadeh M, et al. Curcumin and tamoxifen-loaded nanoparticles for breast cancer cells. BMC Complement Med Ther. 2024; 24:337.
23. Liang H, Zou F, Liu Q, Wang B, Fu L, Liang X, et al. Nanocrystal-loaded liposomes for targeted antitumor drug delivery. Int J Pharm. 2021; 599:120418.
24. Cheng M, Liu Q, Gan T, Fang Y, Yue P, Sun Y, et al. Nanocrystal-loaded micelles for enhanced circulation of docetaxel. Molecules. 2021; 26:4481.
25. Mills JA, Liu F, Jarrett TR, Fletcher NL, Thurecht KJ. Nanoparticle-based medicines: clinical translation and biological barriers. Biomater Sci. 2022; 10:3029-3053.
26. Khan MI, Hossain MI, Hossain MK, Rubel MH, Hossain KM, Mahfuz AM, et al. Recent progress in nanostructured smart drug delivery systems for cancer therapy. ACS Appl Bio Mater. 2022;5:971-1012.
27. Melo MN, Amaral RG, Melo de Andrade LR, Severino P, Blanco-Llamero C, Andrade LN, et al. Randomized phase III clinical trials of cancer nanomedicines. Cancer Pathog Ther. 2024;2:E01-E15.
28. Wang Z, Wang X, Xu W, Li Y, Lai R, Qiu X, et al. Translational challenges in biomimetic delivery systems. Pharmaceutics. 2023; 15:2623.
29. Agrahari V, Agrahari V. Facilitating translation of nanomedicines into clinical products. Drug Discov Today. 2018; 23:974-991.
30. Ioele G, Chieffallo M, Occhiuzzi MA, De Luca M, Garofalo A, Ragno G, et al. Strategies to improve pharmacokinetic and pharmacodynamic properties of anticancer drugs. Molecules. 2022; 27:5436.
31. Gupta R, Chen Y, Xie H. In vitro dissolution considerations associated with nano drug delivery systems. Wiley Interdiscip Rev Nanomed Nanobiotechnol. 2021; 13:e1732.
32. Farkas N, Kramar JA. Dynamic light scattering distributions by any means. J Nanopart Res. 2021; 23:120.
33. Nobbmann U, Connah M, Fish B, Varley P, Gee C, Mulot S, Chen J, Zhou L, Lu Y, Sheng F, Yi J. Dynamic light scattering as a relative tool for assessing the molecular integrity and stability of monoclonal antibodies. Biotechnology and genetic engineering reviews. 2007 Jan 1; 24(1):117-28.
34. Goldstein JI, Newbury DE, Michael JR, Ritchie NW, Scott JH, Joy DC. Scanning electron microscopy and X-ray microanalysis. Springer; 2017 Nov 17.
35. Goikuria U, Larrañaga A, Vilas JL, Lizundia E. Thermal stability increase in metallic nanoparticles-loaded cellulose nanocrystal nanocomposites. Carbohydrate polymers. 2017 Sep 1; 171:193-201.
36. Rasve V, Chakraborty AK, Jain SK, Vengurlekar S. Comparative evaluation of antidiabetic activity of ethanolic leaves extract of Clematis triloba and their SMEDDS formulation in streptozotocin-induced diabetic rats. J Popul Ther Clin Pharmacol. 2022;29(4):959-971. doi:10.53555/jptcp.v29i04.2360.
37. Jiang J, Oberdörster G, Biswas P. Characterization of size, surface charge and agglomeration state of nanoparticle dispersions. J Nanopart Res. 2009; 11:77-89.
38. Bates S, Zografi G, Engers D, Morris K, Crowley K, Newman A. Analysis of amorphous and nanocrystalline solids from XRD. Pharm Res. 2006; 23:2333-2349.
39. Thakral S, Terban MW, Thakral NK, Suryanarayanan R. Characterization of amorphous pharmaceuticals by X-ray diffractometry. Adv Drug Deliv Rev. 2016; 100:183-193.
40. Gil-González E, Perejón A, Sánchez-Jiménez PE, Medina-Carrasco S, Kupčík J, Šubrt J, et al. Crystallization kinetics by XRD and DSC. Cryst Growth Des. 2018; 18:3107-3116.

41. Leyva-Porras C, Cruz-Alcantar P, Espinosa-Solís V, Martínez-Guerra E, Piñón-Balderrama CI, Compeán-Martínez I, et al. Applications of DSC in pharmaceutical research. Polymers. 2020; 12:5.
42. Falsafi SR, Rostamabadi H, Assadpour E, Jafari SM. Morphology and microstructural analysis of nano-carriers. Adv Colloid Interface Sci. 2020; 280:102166.
43. Gupta P, Rai N, Verma A, Gautam V. Microscopy-based methods for characterization and drug delivery. Med Res Rev. 2024; 44:138-168.
44. Lv Y, Wu W, Corpstein CD, Li T, Lu Y. Biological and intracellular fate of drug nanocrystals through different delivery routes. Adv Drug Deliv Rev. 2022; 188:114466.